



BASIC SCIENCE ARTICLE

TLR4 regulates ROS and autophagy to control neutrophil extracellular traps formation against *Streptococcus pneumoniae* in acute otitis media

Yilin Dong¹, Chunfang Jin^{1,2}, Zhiqiang Ding³, Yiting Zhu¹, Qian He¹, Xinxin Zhang¹, Rongshuang Ai¹, Yibing Yin¹ and Yujuan He¹

BACKGROUND: Otitis media (OM), a prevalent pediatric infectious disease, is mainly caused by *Streptococcus pneumoniae* (*S.pn*). Neutrophil extracellular traps (NETs), a novel antimicrobial strategy, were reported in 2004. We found that NETs formed in the middle ear with acute otitis media (AOM) induced by *S.pn*. However, the mechanisms of NETs formation are not entirely clear.

METHODS: We stimulated neutrophils isolated from mouse bone marrow with *S.pn* clinical strain 19F in vitro, and established mouse model of AOM via transbullar injection with *S.pn*. NETs formation, reactive oxygen species (ROS) production, autophagy activation and bacterial load were analyzed in TLR4^{-/-} and wild-type neutrophils stimulated in vitro with *S.pn* and in vivo during AOM.

RESULTS: We found that autophagy and ROS were required for *S.pn*-induced NETs formation. Moreover, TLR4 partly mediated NETs formation in response to *S.pn* in vitro and in vivo during AOM. We also showed that attenuated NETs formation in TLR4^{-/-} neutrophils correlated with an impaired ROS production and autophagy activation in vitro and in vivo. In addition, both the in vivo and in vitro-produced NETs were able to engulf and kill *S.pn*.

CONCLUSIONS: TLR4 regulates ROS and autophagy to control NETs formation against *S.pn* in the course of AOM.

Pediatric Research (2021) 89:785–794; <https://doi.org/10.1038/s41390-020-0964-9>

IMPACT:

- *S.pn* can induce NETs formation in vitro and in vivo; TLR4 regulates NETs formation by ROS and autophagy; NETs contribute to the clearance of bacteria in acute otitis media.
- In this study, we firstly found that autophagy and ROS were required for *S.pn*-induced NETs formation in the model of acute otitis media (AOM). And to some extent, TLR4 mediated NETs formation during AOM.
- Our research might provide a potential strategy for the treatment of otitis media.

INTRODUCTION

Streptococcus pneumoniae (*S.pn*) is a major pathogen of community-acquired pneumonia, meningitis, and otitis media (OM). It was reported that 50% bacteria isolated from middle ear lavage fluid (MELF) of acute otitis media (AOM) patients are *S.pn*.¹ Our previous study demonstrated that neutrophils are the most predominant innate defenders against *S.pn*, which rapidly migrate to middle ear cavity upon infection.² In response to infection, besides phagocytosis and degranulation, a new effector function of neutrophil named neutrophil extracellular traps (NETs) was discovered in 2004.³ NETs, released by activated neutrophils, are highly decondensed web-like DNA structures that are decorated with histones, proteases (e.g. myeloperoxidase, elastase) and antimicrobial peptides (e.g. LL37).⁴ A recent study presented evidence that NETs could function to eliminate *S.pn* in acute and recurrent otitis media.⁵

To date, it is generally accepted that the formation of NETs is dependent on reactive oxygen species (ROS) generation by NADPH oxidase complex.⁶ Inhibitors of this complex abrogate NETs formation in response to various stimuli.⁷ This has been supported by clinical studies on chronic granulomatous disease (CGD) patients, who lack NADPH oxidase activity, and thus fail to form NETs.⁸ Recently, discrepant findings about ROS-independent and/or more complex activation mechanisms emerged. For example, rapid NETs formation, induced by *B. aureus*, is independent on ROS.⁹ Therefore, the mechanisms of NETs formation might vary depending on different stimuli.¹⁰

Autophagy is an intracellular process sequestering and eliminating damaged organelles or proteins to maintain cell survival during starvation and cellular stress.¹¹ An autophagy response can be triggered by various pathogens.¹² Recently, several studies showed that autophagy played an important role in NETs

¹Department of Laboratory Medicine, Key Laboratory of Diagnostic Medicine (Ministry of Education), Chongqing Medical University, Chongqing, People's Republic of China;

²Department of Laboratory Medicine, Chongqing Traditional Chinese Medicine Hospital, Chongqing, People's Republic of China and ³School of Computer Science, Chongqing Institute of Engineering, Chongqing, People's Republic of China

Correspondence: Yujuan He (heyujuan@cqmu.edu.cn)

These authors contributed equally: Yilin Dong, Chunfang Jin

Received: 31 August 2019 Revised: 29 February 2020 Accepted: 29 April 2020

Published online: 21 May 2020

formation,¹³ and pharmacological inhibition of autophagy impaired NETs formation.⁴ In patients with community-acquired pneumonia-induced sepsis and mouse model of sepsis, autophagy primed neutrophils for increased NETs formation.¹⁴ In contrast, McInturff et al.¹⁵ found that autophagy negatively regulated the NETs release induced by LPS. These paradoxical reports indicated that the role of autophagy in NETs formation varied depending on different stimuli or pathological conditions. However, the extent of crosstalk between ROS and autophagy in context of NETs formation remains unclear.

Toll-like receptors (TLRs), serving as pattern recognition receptors (PRRs), recognize the pathogen-associated molecular patterns (PAMPs) of invading bacteria and mediate innate immune responses.¹⁶ There are growing evidences linking the interaction between TLR2/4 and neutrophil functions.¹⁷ Oklu et al.¹⁸ proved that TLR4 modulates the production of NETs in a murine model of hind limb Ischemia-reperfusion (IR) injury. DNA damage-associated molecular pattern protein high-mobility group box 1 (HMGB1) can also induce NETs via TLR4.¹⁹ Additionally, LPS could promote neutrophil autophagy via TLR4.²⁰ Recent study showed that a broad range of TLR2 ligands could efficiently induce ROS-dependent NETs release in young mice, but not in aged ones.²¹ However, it is unclear whether and how TLR2/4 works for the formation of NETs during AOM.

The aim of this study is to investigate whether NETs form during AOM and to further identify the underlying mechanisms. We harvested primary mouse bone-marrow-derived neutrophils and established *S.pn* AOM mouse model by transbullar puncture in WT, TLR2^{-/-} and TLR4^{-/-} mice, and thus to qualitatively and quantitatively measure the formation of NETs. Our data indicated that *S.pn* causes NETs formation in mouse model of AOM. Compared with WT mice, TLR4 deficiency, not TLR2 deficiency, impaired the formation of NETs. Furthermore, *S.pn*-induced NETs formation is dependent on ROS and autophagy, which are mediated, at least in part, by TLR4.

MATERIALS AND METHODS

Mouse model of AOM

The mouse model of AOM was established via transbullar injection according to the method described previously.²² In brief, mice were anesthetized with ketamine hydrochloride (0.020 mg/g of body weight) and xylazine (0.005 mg/g of body weight). A total of 5×10^5 CFU *S.pn* in 5 μ l phosphate buffer saline (PBS) was injected into the middle ear cavity. In some cases, 5 μ l PBS containing 3-Methyladenine (3-MA; 10 mM; Sigma-Aldrich, St. Louis, MO) or diphenylene-iodonium chloride (DPI, 10 μ M, Sigma-Aldrich) and 5×10^5 CFU of *S.pn* was injected. After that, the skin incision was sutured. The following experiments were done in accordance with the Institutional Animal Care and Use Committee's guidelines at Chongqing Medical University.

Isolation and culture of mouse bone-marrow-derived neutrophils
The bone marrow cells were isolated from the tibia and femur of mice. Then the neutrophils were collected according to the manufacturer's instruction of Neutrophil Isolation Kit (mouse; Miltenyi Biotec, Bergisch Gladbach, Germany). The purified cells were seeded into 24-well plates in 10% FBS-RPMI1640 and incubated at 37 °C in a humidified atmosphere containing 5% CO₂ for 2 h.

Microscopy detection of NETs formation

5×10^5 mouse bone-marrow-derived neutrophils were incubated with *S.pn* or Phorbol-12-myristate-13-acetate (PMA) for 0, 0.5, 1, 1.5, 2, 2.5 or 3 h continuously, respectively. Non-cell-permeable DNA dye SYTOX green (Invitrogen, Carlsbad, CA) was used to study the kinetics of NETs formation by fluorescence microscopy.²³ For staining of neutrophil elastase (NE), cells were

permeabilized with 0.5% Triton X-100 at RT for 10 min and incubated with blocking buffer for 1 h at 37 °C. Immunofluorescence was analyzed after overnight incubation with neutrophil elastase antibody (1:800) (Cell Signaling Technology, Danvers, MA), followed by an hour incubation with secondary goat anti-rabbit antibody (1:1000) (Cell Signaling Technology) coupled to Alexa 488, and 4',6-diamidino-2-phenylindole (DAPI) was added for 10 min.

Quantitative detection of NETs formation

Mouse bone-marrow-derived neutrophils were seeded in poly-D-lysine 96-well Flat Clear Bottom Black Polystyrene(Corning, NY) at a density of 1×10^5 cells/well and incubated with or without *S.pn* (at multiplicity of infection, MOI, of 100) or PMA (50 nM) for 0, 0.5, 1, 1.5, 2, 2.5 or 3 h continuously, respectively. At each time point, the plate was gently washed with PBS for three times to remove extracellular *S.pn* or PMA. Subsequently, SYTOX green (5 μ M; excitation: 488 nm, emission: 510 nm) reagent was added into each well and incubated for 15 min at 37 °C in the dark, and the fluorescence of NETs-bound SYTOX green was analyzed by fluorescence spectrophotometer (FLX800 reader). In some cases, mouse bone-marrow-derived neutrophils were pretreated with DPI (10 μ M), 3-MA(10 mM) or DNase I (100U/ml) for 2 h, respectively.

Cell quantification and bacterial load determination

Mice were sacrificed. The tympanic bullae were harvested and split into dorsal and ventral halves. The exposed middle ear (ME) space was lavaged and MELF was collected. To count the pneumococcal numbers, 10 μ l MELF was serially diluted (tenfold) and 10 μ l samples of those dilutions was plated on Columbia sheep blood agar plates. The limit of detection was 10 CFU per ME. Another 10 μ l MELF was added to 190 μ l 1% acetic acid solution for total cell quantification based on standard morphological criteria.

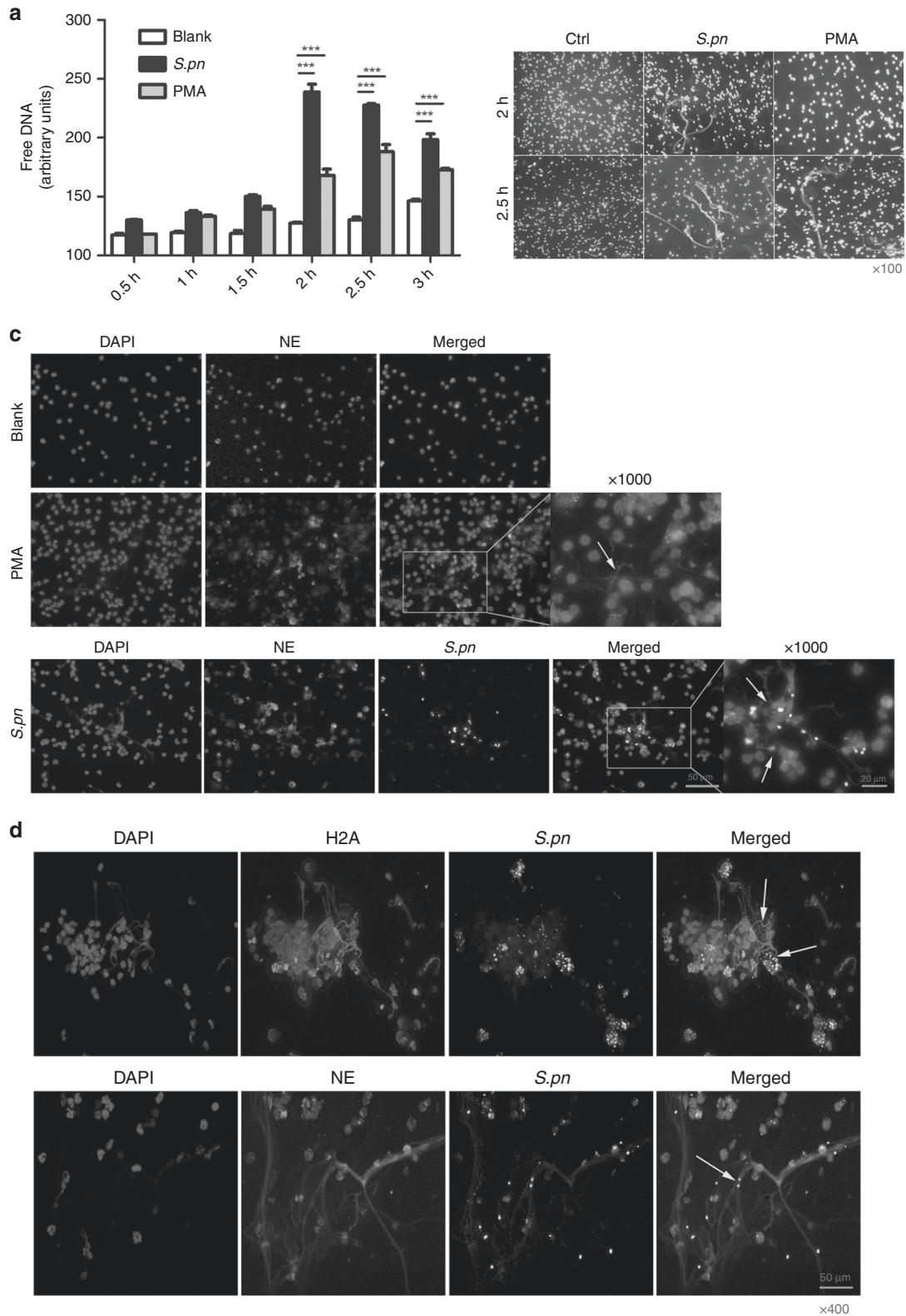
Western blot activated neutrophils were lysed in RIPA buffer (Beyotime Biotechnology, Shanghai, China) supplemented with 1 mM Phenylmethanesulfonyl Fluoride (PMSF). Protein concentrations were determined using BCA protein assay reagent (Beyotime Biotechnology). Twenty micrograms protein was separated in 12% SDS-PAGE, transferred to polyvinylidene fluoride (PVDF) membranes (Millipore, Billerica, MA), and incubated with anti-LC3B antibody (1:1000) and anti-GAPDH (1:5000) (Cell Signaling Technology), and followed by incubation with HRP-coupled secondary antibody (1:10,000) (SeraCare, Gaithersburg, MD).

Confocal microscopy

Isolated mouse bone marrow neutrophils were stimulated with *S.pn* for 2 h. In some cases, neutrophils were pretreated with 10 mM 3-MA or 10 μ M DPI. After fixing with 4% paraformaldehyde for 15 min and permeabilized with 0.5%Triton X-100 at RT for 10 min, cells were incubated with blocking buffer for 1 h. Afterwards, cells were incubated with primary anti-LC3 antibody (1:200) overnight at 4 °C, followed by incubation with secondary goat anti-rabbit antibody coupled to Alexa 488 (1:1000, Cell Signaling Technology) for 1 h at RT, and then DAPI was added for 10 min. Finally, samples were sealed with anti-fade mounting medium.

Determination of ROS production

Total ROS production was measured by fluorescence spectrophotometer (488 nm excitation and 500–600 nm emission, Cary Eclipse) and visualized by fluorescence microscope (Nikon Eclipse 80i, Japan). According to the manufacturer's instructions, neutrophils pretreated with or without *S.pn* for 2 h were incubated in the dark with 10 μ M DCFH-DA (Beyotime Biotechnology, Shanghai, CHINA) at 37 °C for 20 min, and washed with PBS to remove extracellular DCFH-DA, then re-suspended in 200 ml PBS for detection.



NETs killing assay

Neutrophils (2.5×10^5 per well) were seeded in 24-well plates and stimulated with 50 nM PMA for 150 min to induce NETs, following treatment with or without 5 μ g/ml Cytochalasin D (cytD; Chromadex, CA) to inhibit phagocytosis or 100U DNase I to dismantle NETs for 30 min. The plates were centrifuged at

700 \times g for 10 min after adding *S.pn* at a MOI of 1 and then incubated for 30 min at 37 °C. After incubation, supernatants were carefully collected and the cells were lysed in the wells with 500 μ l ice-cold distilled water containing 0.1% Triton X-100 for 20 min and then scraped and pooled with the supernatant. Samples were serially diluted (10^{-1} , 10^{-2} , 10^{-3}) with sterile PBS

Fig. 1 NETs formation induced by *S.pn*. **a** Released extracellular DNA stained by SYTOX green, in response to neutrophils incubation without stimuli (Blank) or with PMA or *S.pn*, from 30 min to 3 h was determined by fluorescence spectrophotometer. Bars are the mean \pm SEM from three independent experiments. *** $P < 0.001$. **b** Extracellular DNA stained by SYTOX green were visualized by fluorescence microscopy after 2 and 2.5 h of neutrophils incubation without stimuli (Blank) or with PMA or *S.pn*. Representative images from three independent experiments are shown. **c** NETs components (blue: DNA; red: neutrophil elastase; green: *S.pn*) were visualized by fluorescence microscopy after 2 h of neutrophils incubation without stimuli (Control) or with *S.pn* or PMA. Representative images from three independent experiments are shown. The extracellular fibers were marked with arrowhead. **d** NETs of middle ears of mice inoculated with *S.pn* were imaged by immunofluorescence for DNA (blue), histone 2A (red, upper panel), NE (red, lower panel) and *S.pn* (green). Representative images from five independent experiments are shown. *S.pn* *Streptococcus pneumoniae*, PMA Phorbol-12-myristate-13-acetate, NE neutrophil elastase, NETs neutrophils extracellular traps.

containing 0.1% Triton X-100, plated on blood plate, and incubated for 24 h at 37 °C to determine the numbers of CFU. Experiments were carried out in triplicate and repeated at least five times.

NETs capture effect assay

FITC-labeled *S.pn* were inactivated in 65 °C water for 30 min. Neutrophils (2.5×10^5 per well) were seeded in 24-well plates and stimulated with 50 nM PMA for 150 min to induce NETs. The plates were washed three times and FITC-labeled inactivated *S.pn* (green) was added. Then plates were incubated for 30 min at 37 °C. Finally, cells were washed three times and NETs marker extracellular DNA was stained with DAPI (blue). The plates were observed under fluorescence microscope.

Statistical analyses

All data were presented as mean \pm SEM. All statistical analyses were performed using Graph-Pad Prism software version 5.01 for Windows (GraphPad, La Jolla, CA). For analysis of CFU data, Mann–Whitney *U* test was performed. For analysis of all other data, unpaired *t* test was performed. $P < 0.05$ was considered statistically significant.

RESULTS

***S.pn* induces NETs formation in mouse primary neutrophils and in mouse model of AOM**

Firstly, activated neutrophils exhibited significantly increased NETs formation in response to *S.pn* 19F, and PMA, a stimulus widely used to activate NETs formation, was used as a positive control (Fig. 1a, b). Furthermore, NETs components were visualized at 2 h post incubation with or without *S.pn* or PMA. As shown in Fig. 1c, the colocalization of extracellular DNA, NE and *S.pn* was observed (Fig. 1c). Given that more than 98% of MELF cells were neutrophils in mouse model of AOM,² we hypothesized that NETs formation took place in middle ear cavity during AOM. As shown in Fig. 1d, immunofluorescence staining confirmed that *S.pn* induced NETs formation in mouse model of AOM. In conclusion, *S.pn* can induce NETs formation in vitro and in vivo.

***S.pn* induces autophagy activation in vitro and in vivo**

To evaluate the production of autophagy in response to *S.pn*, we measured the conversion of autophagy protein LC3-I into LC3-II, which served as a marker of autophagy activation and autophagosome formation. Figure 2a shows a significant increase of LC3-II expression after 30 min post incubation with

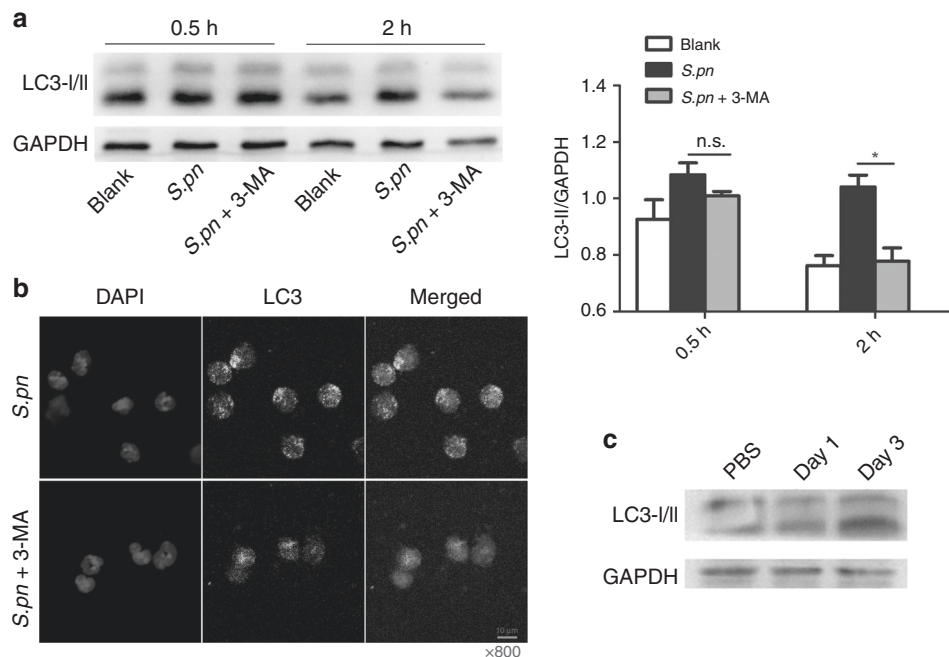


Fig. 2 *S.pn* induced autophagy activation in vitro and in vivo. Neutrophils, pretreated or not with 3-MA (10 mM) for 2 h, were incubated without stimuli (Blank) or with *S.pn* for 30 min or 2 h. **a** The conversions of LC3-I to LC3-II in neutrophils stimulated with *S.pn* were detected by Western blot. Optical density of reactive bands was measured and normalized by the GAPDH density in the same line (right panel). GAPDH was used as loading control. Blots are representative of experiments ($n = 3$) with similar results. Bars are the mean \pm SEM from three independent experiments. * $P < 0.05$. **b** Representative immunofluorescence images for LC3 puncta (green) from five independent experiments with similar results. The middle ear of mice was inoculated with PBS or 5×10^5 CFU *S.pn* for 1 or 3 days and **c** Western blot analysis detected conversion of LC3-I to LC3-II in neutrophils recruited to middle ear cavity. Representative images from four independent experiments are shown. 3-MA 3-Methyladenine.

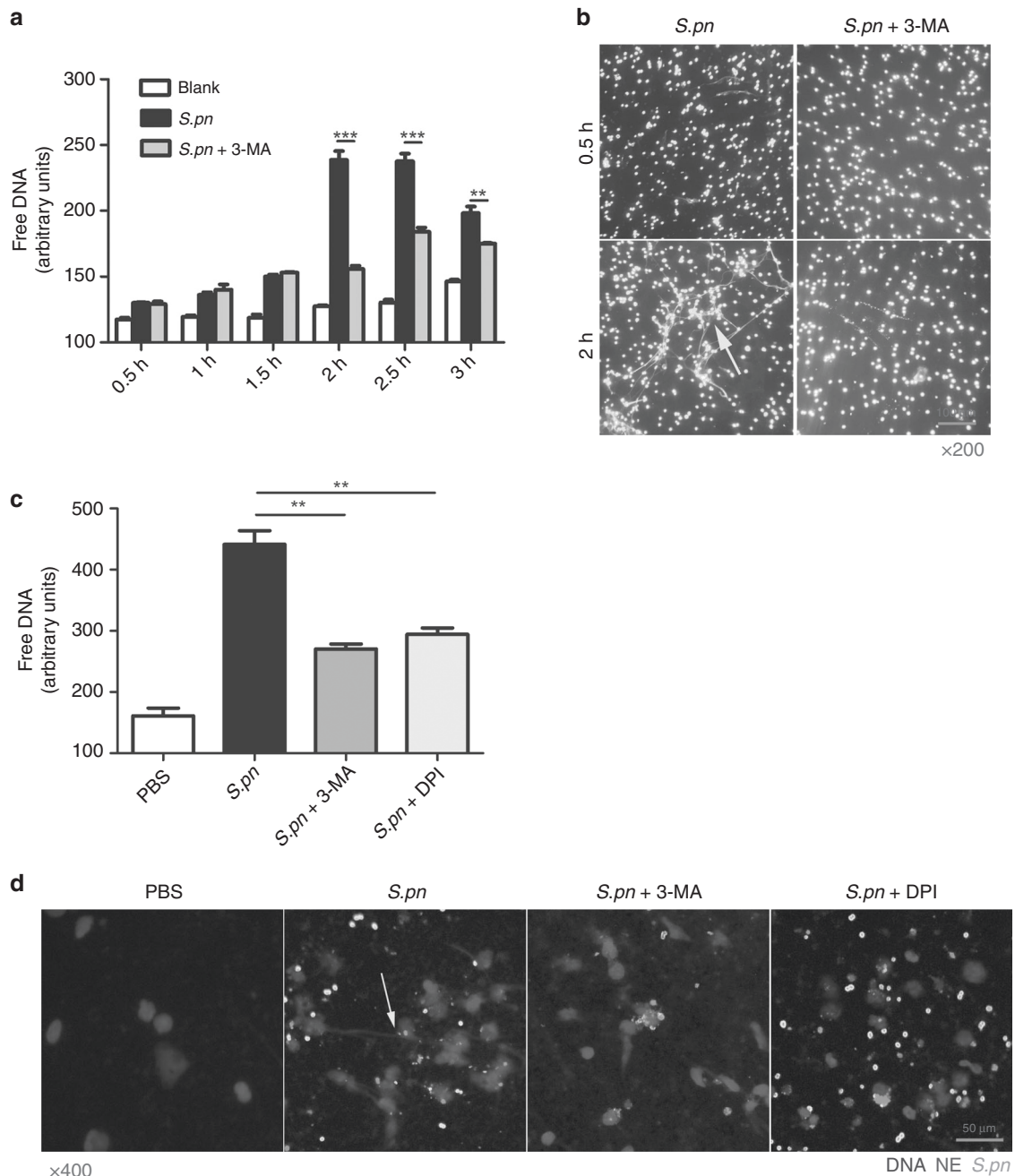


Fig. 3 NETs formation induced by *S.pn* depends on autophagy. Neutrophils, pretreated or not with 3-MA (10 mM) for 2 h, were incubated without stimuli (blank) or with *S.pn* from 30 min to 3 h, and **a** fluorospectrophotometry for extracellular free DNA and **b** representative immunofluorescence images for NETs structure were measured as described in "Materials and Methods". Bars are the mean \pm SEM from three independent experiments. ** $P < 0.01$, *** $P < 0.001$. The middle ear of mice was inoculated with PBS (Blank), 5×10^5 CFU *S.pn* alone, *S.pn* plus 3-MA, or *S.pn* plus DPI for 1 day. **c** Extracellular free DNA of MELF was measured by fluorospectrophotometry. Bars are the mean \pm SEM from four independent experiments. ** $P < 0.01$. **d** NETs components (blue, DNA; red, NE; green, *S.pn*) in the smear of MELF were visualized by fluorescence microscopy. Representative images from four independent experiments are shown. DPI diphenylene-iodonium chloride, MELF middle ear lavage fluid.

S.pn. In addition, following *S.pn* infection, there was a significant increase in the numbers of LC3 puncta per cell (Fig. 2b). Then treatment of neutrophils with 3-MA, a well-known autophagy inhibitor, significantly inhibited the conversion of LC3-I to LC3-II and abrogated the production of LC3 puncta (Fig. 2a, b). Consistently, the expression of LC3-II is significantly increased on days 1 and 3 post incubation with *S.pn* in mouse model of AOM (Fig. 2c).

NETs formation induced by *S.pn* depends on autophagy
We evaluated whether autophagy induced by *S.pn* regulated NETs formation. Pretreated with 3-MA, neutrophils showed a significant reduction of NETs formation in response to *S.pn* after 2 h (Fig. 3a, b). We next examined whether autophagy induced by *S.pn* regulated NETs formation in mouse model of AOM. Firstly, neutrophils were the predominant effector cells (>98%) analyzed by FCM (data not shown), and there was no statistically significant difference in the

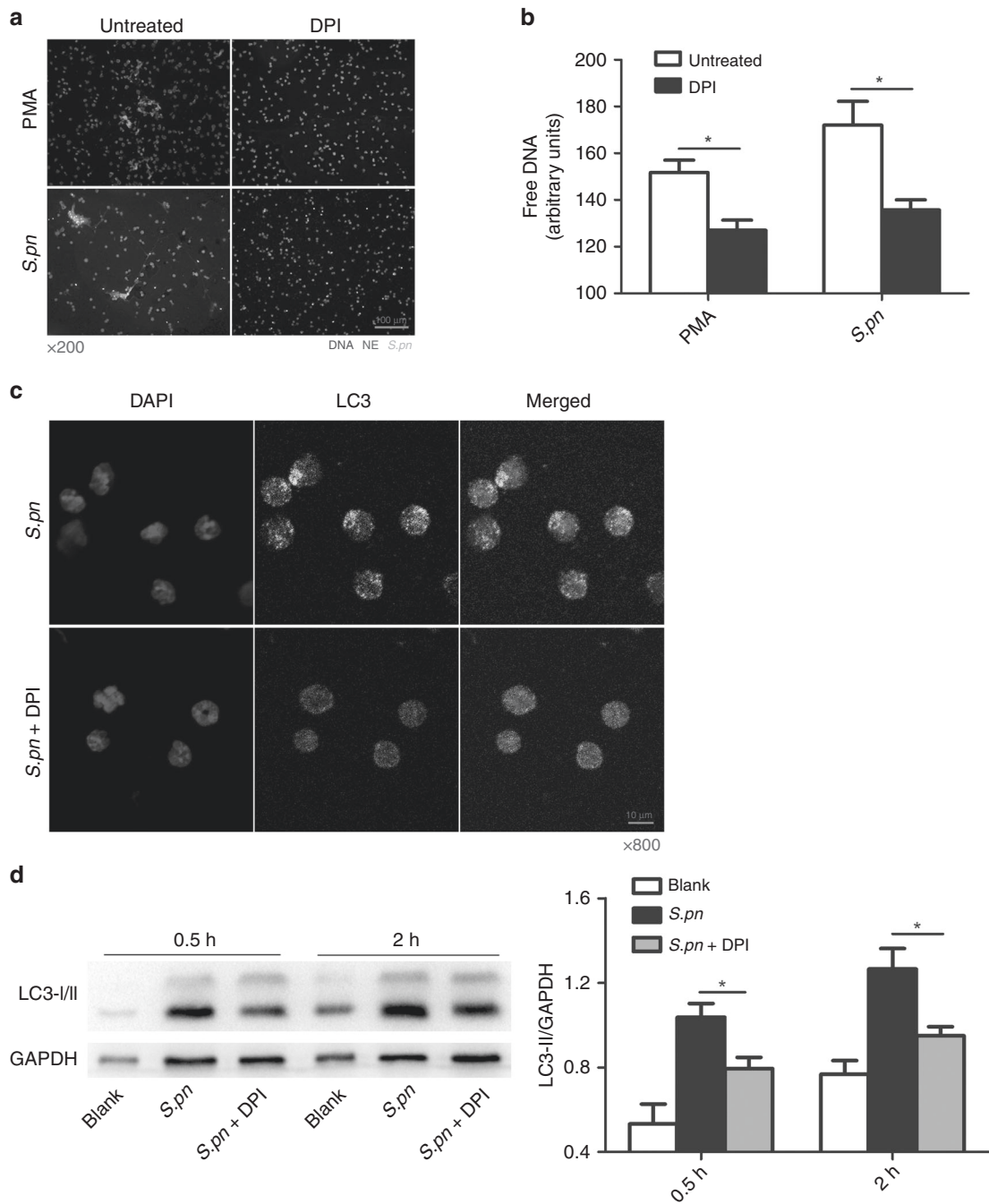


Fig. 4 ROS induces NETs formation via regulating autophagy. Neutrophils, pretreated or not with DPI (10 μ M) for 2 h, were incubated with PMA or *S.pn* for 2 h. **a** Representative immunofluorescence images for NETs components (blue, DNA; red, NE; green, *S.pn*) are shown from four independent experiments. **b** Fluorospectrophotometry for extracellular free DNA. Bars are the mean \pm SEM from three independent experiments. $*P < 0.05$. **c** Representative immunofluorescence images for LC3 puncta. Representative immunofluorescence images are shown from four independent experiments. **d** Western blot analysis for the conversions of LC3-I to LC3-II in neutrophils. Optical density of reactive bands was measured and normalized by the GAPDH density in the same line (right panel). GAPDH was used as internal control. Blots are representative of experiments ($n = 3$) with similar results.

amounts of neutrophils after treated with 3-MA simultaneously (Supplementary Fig. S1). Compared with *S.pn*-treated group, the extracellular free DNA at 24 h post infection was significantly decreased in *S.pn* plus 3-MA-treated group (Fig. 3c), suggesting that the ability of NETs formation in the middle ear of mice was significantly reduced after inhibition of autophagy. Furthermore, as shown in Fig. 3d, inhibition of autophagy attenuated NETs formation in mouse model of AOM. Taken together, NETs formation induced by *S.pn* depends, at least in part, on autophagy.

ROS induces NETs formation via regulating autophagy

Our previous study has demonstrated that ROS production is significantly increased when neutrophils are stimulated by *S.pn*, and it can be markedly inhibited by DPI pretreatment.²⁴ To verify whether NETs formation depends on ROS production, we incubated neutrophils with DPI. The results showed that DPI not only reduced DNA fiber structure formation (Fig. 4a), but also significantly reduced the amounts of extracellular free DNA (Fig. 4b). Our previous study has demonstrated that DPI

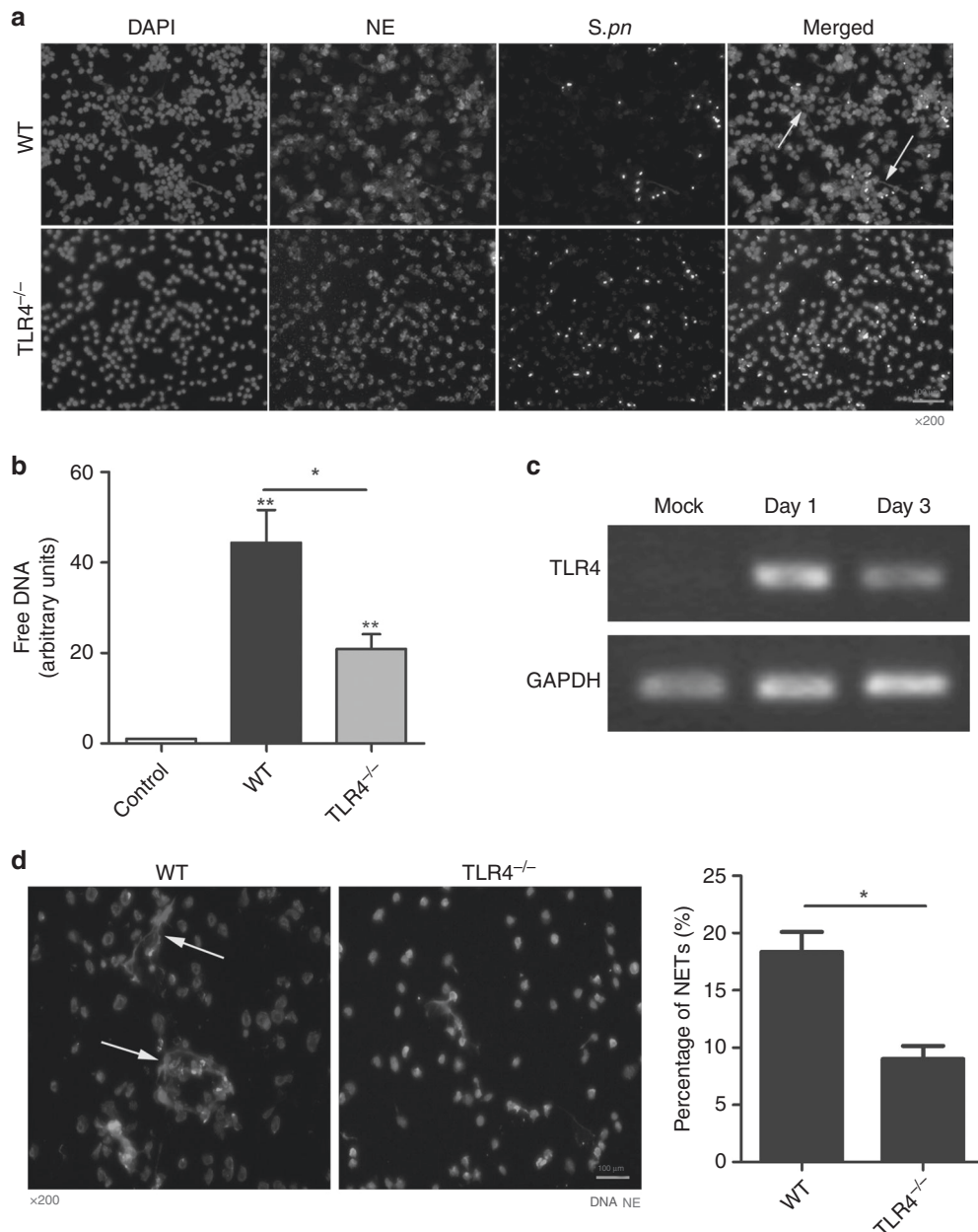


Fig. 5 TLR4 deficiency causes impairment of NETs formation. Neutrophils derived from wild-type or TLR4^{-/-} mice were incubated with *S.pn* for 2 h. **a** Representative immunofluorescence images for NETs components (blue, DNA; red, NE; green, *S.pn*) are shown from four independent experiments. **b** Fluorospectrophotometry for extracellular free DNA. Bars are the mean ± SEM from three independent experiments. ***P* < 0.01. The mouse model of AOM was established in wild-type mice and TLR4^{-/-} mice, respectively. The middle ear of mice was inoculated with PBS (control) or 5 × 10⁵ CFU *S.pn* for 1 or 3 days. **c** TLR4 mRNA expression in middle ear epithelium of wild-type mice was analyzed by PCR. **d** NETs components (blue, DNA; red, NE. Left panel) in the smear of MELF were visualized by fluorescence microscopy and percentages of NETs cells were counted (Right panel). Data are representative of experiments (*n* = 3–5) with similar results, **P* < 0.05.

administration did not affect the types and amounts of recruited cells in MELF.²⁵ In the presence of DPI, the extracellular free DNA and DNA fiber structures were significantly decreased (Fig. 3c, d). These results suggested that ROS production is a crucial mediator of NETs formation in vitro and in vivo.

Next, we tested whether inhibition of ROS by DPI could reverse the activation of autophagy. Immunofluorescence staining of LC3 showed a homogenous distribution of LC3 in the cytoplasm with DPI treatment (Fig. 4c), suggesting that inhibition of ROS significantly attenuated activation of autophagy. Western blot analysis further confirmed attenuated activation of autophagy in the presence of DPI, in comparison with their untreated

counterparts (Fig. 4d). Taken together, these data suggest that ROS may promote NETs formation by activating autophagy.

TLR4 deficiency causes impairment of NETs formation

It has been reported that TLR2 and TLR4 may be involved in NETs formation; thus, we evaluated whether TLR2 or TLR4 regulated NETs formation. Neutrophils isolated from WT, TLR2^{-/-} and TLR4^{-/-} mouse bone marrow, respectively, were stimulated with *S.pn* for 2 h. Compared with WT neutrophils, TLR4^{-/-} neutrophils exhibited significantly reduced NETs formation in response to *S.pn* (Fig. 5a, b). However, there is no statistically significant difference between the WT and TLR2^{-/-} groups (data not shown). Next, we

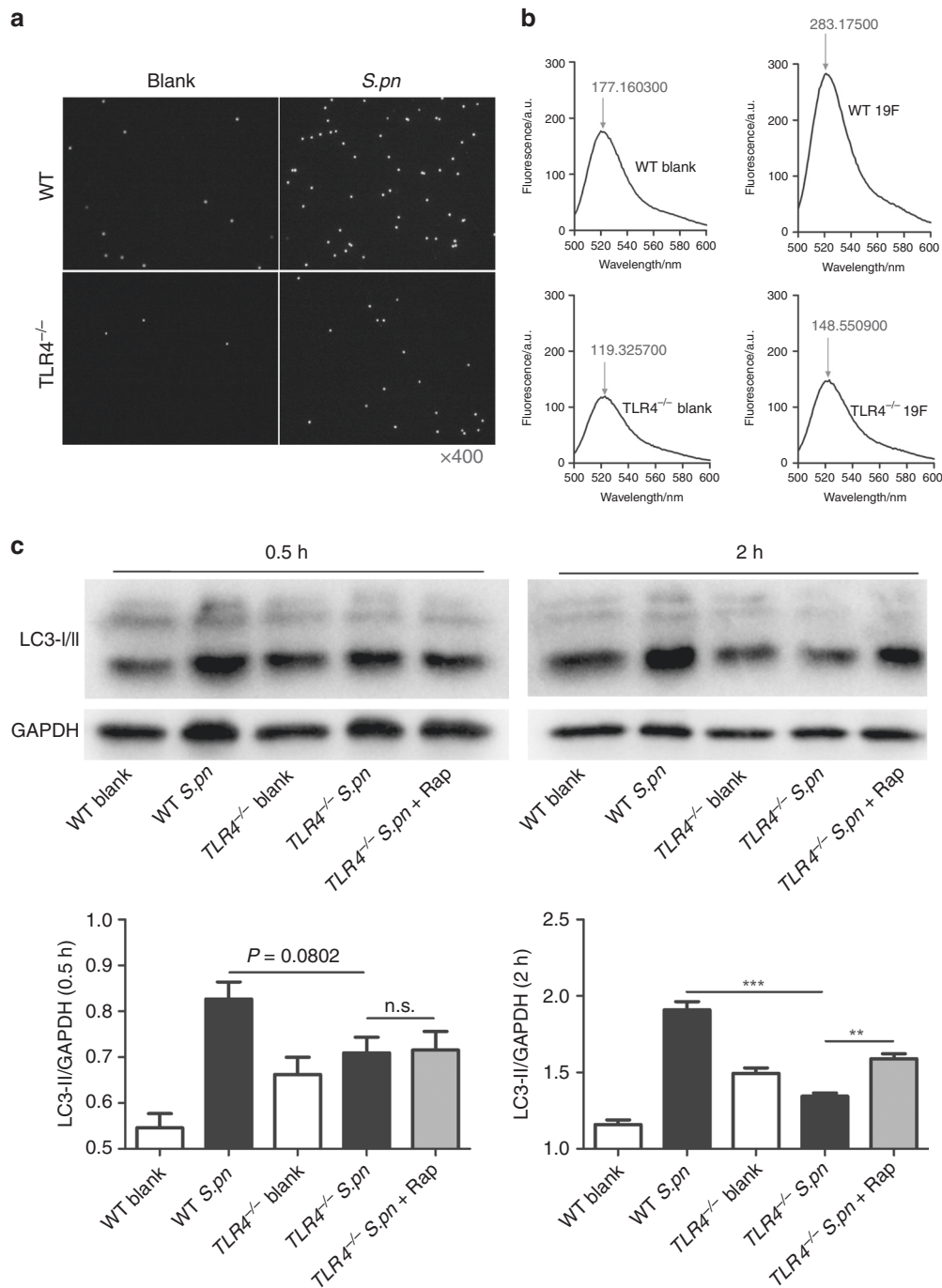


Fig. 6 TLR4 deficiency reduces ROS production and impairs autophagy activation. Neutrophils derived from wild-type or TLR4^{-/-} mice were incubated with *S.pn* for 2 h. **a** Representative fluorescence images show the production of ROS and **b** quantification of fluorescence intensity of ROS was measured by fluorospectrophotometry. Neutrophils from wild-type or TLR4^{-/-} mice pretreated or not with rapamycin (1 μM) for 2 h were incubated without stimuli (blank) or with *S.pn* for 30 min or 2 h and **c** Western blot analysis detected conversion of LC3-I to LC3-II in neutrophils (upper panel). Optical density of reactive bands was measured and normalized by the GAPDH density in the same line (lower panel). GAPDH was used as loading control. Blots are representative of experiments ($n = 3$) with similar results. ROS reactive oxygen species.

examined whether TLR4 involved in NETs formation in vivo. We first confirmed that the expression of TLR4 increased in mouse middle ear tissue after infection with *S.pn* for 24 h (Fig. 5c). Immunofluorescence staining suggested that DNA fiber structures significantly decreased in TLR4^{-/-} mice compared with WT mice (Fig. 5d, left panel). Consistently, the percentage of NETs cells is significantly reduced in TLR4^{-/-} mice (Fig. 5d, right panel). These findings indicated TLR4 was critical for NETs formation in AOM.

TLR4^{-/-} deficiency reduces ROS production and impairs autophagy activation
Considering the well-established contributions of ROS and autophagy in NETs formation induced by *S.pn*, we analyzed whether impaired NETs formation in TLR4^{-/-} neutrophils was due to the defects in ROS production and autophagy activation. Fluorescence microscopy displayed a significant decrease of ROS production in TLR4^{-/-} neutrophils at 2 h post infection by *S.pn*

(Fig. 6a). Consistently, TLR4 deficiency caused a dramatic decrease of fluorescence intensity by ROS assay kit (Fig. 6b), indicating a significant reduction of ROS production. Western blot analysis confirmed that autophagy activation was attenuated in TLR4^{-/-} neutrophils at 2 h post infection by *S.pn*, which was partly rescued by rapamycin, an inducer of autophagocytic vacuole formation via inhibiting the mTOR signal pathway (Fig. 6c). These data implied that ROS and autophagy played critical roles in TLR4-mediated NETs formation.

NETs capture and kill *S.pn*

To investigate whether NETs capture *S.pn*, we visualized the trapping of *S.pn* treated with or without DNase I, which degrades extracellular DNA. In the presence of DNase I, fibroid DNA significantly diminished and FITC-labeled inactivated *S.pn* scattered homogenously. While in the absence of DNase I, inactivated *S.pn* accumulated to the sites of extracellular DNA (Supplementary Fig. S2), suggesting *S.pn* was indeed captured by NETs. Next, we assessed the killing effect of NETs on *S.pn*. To distinguish the bactericidal effect between phagocytosis and NETs, we used CytD, an actin polymerization inhibitor, to block phagocytosis, and DNase I to block NETs formation respectively. The results showed that the capacity of NETs-mediated killing was significantly reduced after DNase I treatment, while the capacity of phagocytosis-mediated killing was also significantly reduced after treatment with CytD (Supplementary Fig. S3), suggesting that both NETs and phagocytosis played a role in killing *S.pn*.

Next, we explored whether NETs contribute to bactericidal effect in AOM induced by *S.pn*. We firstly confirmed that DNase I administration did not affect the types (data not shown) and amounts of recruited cells in MELF (Supplementary Fig. S4). Compared with DNase I-untreated mice, bacterial load increased in DNase I-treated mice, as well as extracellular free DNA in MELF significantly decreased (Supplementary Figs. S5, S6). We also found that neither 3-MA nor DPI administration affected the types (data not shown) and amounts of recruited cells in MELF (Supplementary Fig. S7). Compared with *S.pn*-treated mice, we observed significant increase of bacterial load in MELF of *S.pn* plus 3-MA-treated mice, and merely increase the tendency of bacterial load in MELF of *S.pn* plus DPI-treated mice, suggesting that autophagy-mediated NETs make more contribution to *S.pn* clearance than ROS-mediated NETs in vivo (Supplementary Fig. S8).

DISCUSSION

In this study, we demonstrated that both autophagy and ROS are required for NETs formation in AOM induced by *S.pn*. In addition, TLR4 contributed to the regulation of NETs formation via autophagy activation and ROS production. We also demonstrated that NETs served as an important antimicrobial strategy of neutrophils against *S.pn* during AOM.

NETs formation is known to be stimulated by PMA, some cytokines, bacterial products and, importantly, by clinically relevant bacteria and fungi.²⁵ In chinchilla model of chronic pneumococcal otitis media, Reid et al.²⁶ confirmed that *S.pn* TIGR4 induced biofilms and NETs formation in middle ear effusions. Antibodies facilitated the development of secondary bacterial OM by inducing NETs in the middle ear of mouse with OM.²⁷ In addition, recent studies on children with chronic otitis media also showed that NETs are macromolecular constituents of middle ear effusions.⁵ Similarly, our study firstly confirmed that *S.pn* 19F induced NETs formation in mouse model of AOM. TLRs recognize the PAMPs of invading bacteria and mediate innate immune responses for host defense.¹⁶ Some studies have shown that various TLRs, including TLR2, TLR4, TLR7, TLR8 and TLR9, can mediate NETs formation.^{19,28–30} Our study demonstrated, for the first time, that TLR4 was required for NETs formation in AOM mouse model.

The mechanism underlying the control of NETs formation following interaction with pathogenic bacteria is still not entirely clear. A key intermediate required for NETs is the production of reactive oxygen intermediates. This view has been supported by clinical studies on CGD patients.⁸ ROS, stimulated by various agents, are required for the release of NE from azurophilic granules into the cytoplasm, a pre-requisite for its translocation to the nucleus. Consequently, elastase mediates the breakdown of chromatin by cleaving histones, leading to the formation of NETs.³¹ However, many discrepant findings were reported that rapid NETs formation (within minutes) induced by *S. aureus*, MSU crystals or calcium did not require ROS production, suggesting ROS-mediated signaling is not the only way to trigger NETs release.^{32,33} In our study, we confirmed that NETs release induced by *S.pn* 19F is dependent on ROS. We speculated that the mechanisms of NETs formation might vary depending on different stimuli and stages.

Recently, several studies have shown that pharmacological inhibition of autophagy impaired NETs formation, suggesting that autophagy plays an important role in NETs formation.¹³ In patients with community-acquired pneumonia-induced sepsis and mouse model of sepsis, autophagy primes neutrophils for increased NETs formation.¹⁵ Previously, Chargui et al.³⁴ identified the link between autophagy and NETs in autophagy-deficient PLB Sh-atg5 cells, and confirmed that NETs took place after autophagy. Furthermore, Li's group³⁵ showed that histone hypercitrullination catalyzed by peptidylarginine deiminase 4 is essential for chromatin decondensation during NETs formation. Here, we also validated that NETs release induced by *S.pn* 19F is dependent on autophagy.

It has been shown that PMA-induced NETs formation requires both autophagy and ROS generation, and inhibition of either autophagy or NADPH oxidase activity prevents NETs formation, implying both of them are indispensable.⁴ However, our results showed that ROS and autophagy are independent inducers of NETs formation. Indeed, several studies showed that ROS mediates autophagy process.³⁶ ROS possibly acts downstream of autophagy activation because Mincle^{-/-} neutrophils are defective in NETs formation despite the production of ROS, due to impaired autophagy, which demonstrated a pivotal role of Mincle in activation of autophagy independent of the ROS pathway.³⁷ This provided an opportunity to dissect the molecular events underlying these two pathways independently of each other.

In 2004, NETs as a novel antimicrobial strategy of neutrophils were reported.³ NETs can trap and kill extracellular pathogens by placing them in close proximity to antimicrobial components. However, some studies on pneumococcal interactions with NETs confirmed that *S.pn* was captured but not killed by NETs. For instance, Beiter et al.³⁸ found that *S.pn* surface endonuclease EndA can degrade the DNA skeleton of NETs, and thereby evade the capture and bactericidal action of NETs. Wartha et al.³⁹ showed that capsule and D-alanylated lipoteichoic acids protect *S.pn* against NETs. Herein, we confirmed that NETs not only captured but killed *S.pn* in vitro and in vivo. Considering its structural characteristics, the bactericidal action of NETs should be undeniable. Therefore, we hypothesize that the outcome of bacterial load depends on the context where the specific evading strategy of *S.pn* competes with the bactericidal capacity of NETs. In our study, we validated that both NETs and phagocytosis displayed bactericidal capability in AOM induced by *S.pn* 19F.

In summary, the present study revealed a complex set of regulatory mechanisms, including the autophagy and ROS, underlying NETs formation in activated human neutrophils. As the capability of neutrophils to combat against infection is not limited to NETs release (i.e. degranulation, phagocytosis), future studies will be focused on elucidating the missing links explaining how neutrophils have evolved a strategy for pathogen clearance in response to *S.pn* infection.

ACKNOWLEDGEMENTS

This work was supported by the National Natural Science Foundation Grants of China (No. csc81373151) and Natural Science Foundation Project of CQCSTC (Nos. cstc2012jjA0035, cstc2018jcyjAX0257).

AUTHOR CONTRIBUTIONS

Y.H. and Y.D. conceived of and designed the research. Y.D., C.J., Y.Z., Q.H., X.Z. and Z.D. performed the experiments and analyzed the data. Y.H., Z.D. and Y.D. wrote the manuscript. R.A. and Y.Y. interpreted the data.

ADDITIONAL INFORMATION

The online version of this article (<https://doi.org/10.1038/s41390-020-0964-9>) contains supplementary material, which is available to authorized users.

Competing interests: The authors declare no competing interests.

Publisher's note Springer Nature remains neutral with regard to jurisdictional claims in published maps and institutional affiliations.

REFERENCES

1. Taylor, S., Marchisio, P. & Vergison, A. Impact of pneumococcal conjugate vaccination on otitis media: a systematic review. *Clin. Infect. Dis.* **54**, 1765–1773 (2012).
2. Wang, W., Zhou, A. & Zhang, X. Interleukin 17A promotes pneumococcal clearance by recruiting neutrophils and inducing apoptosis through a p38 mitogen-activated protein kinase-dependent mechanism in acute otitis media. *Infect. Immun.* **82**, 2368–2377 (2014).
3. Brinkmann, V. Neutrophil extracellular traps kill bacteria. *Science* **303**, 1532–1535 (2004).
4. Remijsen, Q., Berghe, T. V. & Wirawan, E. Neutrophil extracellular trap cell death requires both autophagy and superoxide generation. *Cell Res.* **21**, 290–304 (2011).
5. Schachern, P. A., Kwon, G. & Briles, D. E. Neutrophil extracellular traps and fibrin in otitis media: analysis of human and chinchilla temporal bones. *JAMA Otolaryngol. Head Neck Surg.* **143**, 990–995 (2017).
6. Stoiber, W., Obermayer, A. & Steinbacher, P. The role of reactive oxygen species (ROS) in the formation of extracellular traps (ETs) in humans. *Biomolecules* **5**, 702–723 (2015).
7. Kirchner, T., Möller, Sonja & Klinger, M. The impact of various reactive oxygen species on the formation of neutrophil extracellular traps. *Mediators Inflamm.* **2012**, 849136 (2012).
8. Yost, C. C., Cody, M. J. & Harris, E. S. Impaired neutrophil extracellular trap (NET) formation: a novel innate immune deficiency of human neonates. *Blood* **113**, 6419–6427 (2009).
9. Van Avondt, Van dLM & Naccache, P. H. Signal inhibitory receptor on leukocytes-1 limits the formation of neutrophil extracellular traps, but preserves intracellular bacterial killing. *J. Immunol.* **196**, 3686–3694 (2016).
10. Kenny, E. F., Herzig, A. & Renate, Krüger Diverse stimuli engage different neutrophil extracellular trap pathways. *Elife* **6pii**, e24437 (2017).
11. Nakagawa, I., Amano, A. & Mizushima, N. Autophagy defends cells against invading group A Streptococcus. *Science* **306**, 1037–1040 (2004).
12. Jones, S. A., Mills, K. H. & Harris, J. Autophagy and inflammatory diseases. *Immunol. Cell Biol.* **91**, 250–258 (2013).
13. Itakura, A. & Mccarty, O. J. T. Pivotal role for the mTOR pathway in the formation of neutrophil extracellular traps via regulation of autophagy. *Am. J. Physiol. Cell Physiol.* **305**, C348–C354 (2013).
14. Park, S. Y., Shrestha, S. & Youn, Y. J. Autophagy primes neutrophils for neutrophil extracellular trap formation during sepsis. *Am. J. Respir. Crit. Care Med.* **196**, 577–589 (2017).
15. Mcinturff, A. M., Cody, M. J. & Elliott, E. A. Mammalian target of rapamycin regulates neutrophil extracellular trap formation via induction of hypoxia-inducible factor 1 α . *Blood* **120**, 3118–3125 (2012).
16. Kumar, H., Kawai, T. & Akira, S. Toll-like receptors and innate immunity. *Biochem. Biophys. Res. Commun.* **388**, 621–625 (2009).

17. Sabroe, I., Prince, L. R. & Jones, E. C. Selective roles for Toll-like receptor (TLR)2 and TLR4 in the regulation of neutrophil activation and life span. *J. Immunol.* **170**, 5268–5275 (2003).
18. Oklu, R., Albadawi, H. & Jones, J. E. Reduced hind limb ischemia-reperfusion injury in Toll-like receptor-4 mutant mice is associated with decreased neutrophil extracellular traps. *J. Vasc. Surg.* **58**, 1627–1636 (2013).
19. Tadie, J. M., Bae, H. B. & Jiang, S. HMGB1 promotes neutrophil extracellular trap formation through interactions with Toll-like receptor 4. *Am. J. Physiol. Lung Cell Mol. Physiol.* **304**, L342–L349 (2013).
20. Mitroulis, I., Kourtzelis, I. & Kambas, K. Regulation of the autophagic machinery in human neutrophils. *Eur. J. Immunol.* **40**, 1461–1472 (2010).
21. Xu, F., Zhang, C. & Zou, Z. Aging-related Atg5 defect impairs neutrophil extracellular traps formation. *Immunology* **151**, 417–432 (2017).
22. Huang, Y., Wang, Z. & Jin, C. TLR2 promotes macrophage recruitment and S. pneumoniae clearance during mouse otitis media. *Pediatr. Res.* **80**, 886–893 (2016).
23. Allen, L. A. Immunofluorescence and confocal microscopy of neutrophils. *Methods Mol. Biol.* **1124**, 251–268 (2014).
24. Xiang, Y., Jin, C. & Wang, W. The critical role of myeloperoxidase in streptococcus pneumoniae clearance and tissue damage during mouse acute otitis media. *Innate Immun.* **23**, 296–306 (2017).
25. Urban, C. F., Reichard, U. & Brinkmann, V. Neutrophil extracellular traps capture and kill *Candida albicans* yeast and hyphal forms. *Cell Microbiol.* **8**, 668–676 (2010).
26. Reid, S., Hong, W. & Dew, K. Streptococcus pneumoniae forms surface-attached communities in the middle ear of experimentally infected chinchillas. *J. Infect. Dis.* **199**, 786–794 (2009).
27. Short, K. R., von Köckritz-Blickwede, M. & Langereis, J. D. Antibodies mediate formation of neutrophil extracellular traps in the middle ear and facilitate secondary pneumococcal otitis media. *Infect. Immun.* **82**, 364–370 (2014).
28. Ma, Y. H., Ma, T. & Wang, C. High-mobility group box 1 potentiates antineutrophil cytoplasmic antibody-inducing neutrophil extracellular traps formation. *Arthritis Res Ther.* **18**, 2 (2016).
29. Saitoh, T., Komano, J. & Saitoh, Y. Neutrophil extracellular traps mediate a host defense response to human immunodeficiency virus-1. *Cell Host Microbe* **12**, 109–116 (2012).
30. Huang, H., Tohme, S. & Alkhafaji, A. B. Damage-associated molecular pattern-activated neutrophil extracellular trap exacerbates sterile inflammatory liver injury. *Hepatology* **62**, 600–614 (2015).
31. Metzler, K., Goosmann, C. & Lubojemska, A. A myeloperoxidase-containing complex regulates neutrophil elastase release and actin dynamics during NETosis. *Cell Rep.* **8**, 883–896 (2014).
32. Arai, Y., Nishinaka, Y. & Arai, T. Uric acid induces NADPH oxidase-independent neutrophil extracellular trap formation. *Biochem. Biophys. Res. Commun.* **443**, 556–561 (2014).
33. Pilszczek, F. H., Salina, D. & Poon, K. K. H. A novel mechanism of rapid nuclear neutrophil extracellular trap formation in response to *staphylococcus aureus*. *J. Immunol.* **185**, 7413–7425 (2010).
34. Chargui, A., Cesaro, A. & Mimouna, S. Subversion of autophagy in adherent invasive escherichia coli-infected neutrophils induces inflammation and cell death. *PLoS ONE* **7**, e51727 (2012).
35. Li, P., Li, M. & Lindberg, M. R. PAD4 is essential for antibacterial innate immunity mediated by neutrophil extracellular traps. *J. Exp. Med.* **207**, 1853–1862 (2010).
36. Dewaele, M., Maes, H. & Agostinis, P. ROS-mediated mechanisms of autophagy stimulation and their relevance in cancer therapy. *Autophagy* **6**, 838–854 (2010).
37. Sharma, A., Simonson, T. J. & Jondle, C. N. Mincle-mediated neutrophil extracellular trap formation by regulation of autophagy. *J. Infect. Dis.* **215**, 1040–1048 (2017).
38. Beiter, K., Wartha, F. & Albiger, B. An endonuclease allows streptococcus pneumoniae to escape from neutrophil extracellular traps. *Curr. Biol.* **16**, 401–407 (2006).
39. Wartha, F., Beiter, K. & Albiger, B. Capsule and d-alanylated lipoteichoic acids protect *Streptococcus pneumoniae* against neutrophil extracellular traps. *Cell Microbiol.* **9**, 1162–1171 (2010).